Generalized Excess Noise Factor for Avalanche Photodiodes of Arbitrary Structure

NAGIB Z. HAKIM, STUDENT MEMBER, IEEE, BAHAA E. A. SALEH, SENIOR MEMBER, IEEE, AND MALVIN C. TEICH, FELLOW, IEEE

Abstract—**The output current of an avalanche photodiode (APD) fluctuates in the absence of light as well as in its presence. The noise in this current arises from three sources: randomness in the number and in the positions at which dark carrier pairs are generated, randomness in the photon arrival number, and randomness in the carrier multiplication process. The volume dark current in many multilayer and conventional APD's, unlike the current arising from injected carriers, results from thermal or tunneling processes that generate electron–hole pairs randomly throughout the depletion region of the device. This results in a smaller mean multiplication and a larger excess noise factor than the usual values associated with carriers injected at one edge of the depletion region. Photogenerated carriers produced by light incident on the depletion region are also subject to this modified multiplication. We consider a generic model for a multilayer avalanche photodiode that admits arbitrary variation (with position) of the bandgap, dark generation rate, and ionization coefficients within each stage of the device. Expressions for the mean multiplication and excess noise factors for dark carriers alone, injected carriers alone, and for an arbitrary superposition of dark and injected carriers are derived for this general model. Special cases of our results reduce to well known expressions for the conventional APD, the separate absorption/grading/multiplication APD, the multiquantum-well APD, and the staircase APD.**

I. Introduction

THE output current of an avalanche photodiode (APD) fluctuates in the absence of light as well as in its presence. The noise in this current arises from three sources: randomness in the number and in the positions at which dark carrier pairs are generated, randomness in the photon arrival number, and randomness in the carrier multiplication process. General results are available for the variance of the photodetector output current in terms of the photon-number variance-to-mean ratio for the light and the excess noise factor for the detector in the absence of dark events [1]. The output-current variance has been shown to be directly proportional to the detector excess noise factor when the number of photons at the input to the detector is Poisson distributed. Explicit expressions for the excess noise factor are available for both double-carrier-multiplication conventional APD's (CAPD's) [2], [3] and double-carrier-multiplication multilayer (superlattice) APD's [1]. The results for the special case of a single-carrier multilayer APD agree with those reported by Capasso *et al.* [4] for the graded-gap staircase APD. The excess noise factor is a useful quantity because it compactly represents the statistical properties of the gain fluctuations that introduce multiplicative noise.

In many applications involving the detection of light, the absorption of photons is localized in a certain region of the device external to the multiplication region so that all of the photocarriers enter this region at its edge and thereby have an opportunity to experience the same multiplication. However, in the presence of dark current, this is generally not the case. The electron–hole pairs constituting the bulk dark current are generated throughout the bulk of the material so that most of them will be partially multiplied rather than fully multiplied, as has long been known [5]. Because of the randomness in the locations of these generations, the mean multiplication is smaller, and the excess noise factor larger, than the usual values associated with injected carriers [6]–[8]. Photogenerated carriers resulting from light that happens to be absorbed in the depletion region of the device also undergo partial multiplication.

Dark noise in APD's usually comprises both a nonmultiplied part (usually ascribed to surface leakage) and a multiplied part (the bulk dark current) [5], [9]. The nonmultiplied part, which in some devices far exceeds the multiplied part [5], is taken to arise from Poisson events and is therefore taken to result in shot noise in the circuit of the device. Most experimental studies of APD dark current have focused on the behavior of its mean value as a function of reverse-bias voltage or temperature [10] (and see, for example, [11] and [12]). However, the entire APD dark-current electron counting distribution has been measured in a few studies (see, for example, [13]–[15]). Of course, the latter results contain more information than just the mean value alone.

In this paper, we consider a generic multilayer avalanche photodiode model in which carrier transport takes place perpendicularly to the plane of the layers. Our structure admits arbitrary variations (with position) of the bandgap, dark generation rate, and ionization coefficients

Manuscript received April 8, 1989; revised August 20, 1989. This research was supported by the National Science Foundation. The review of this paper was arranged by Associate Editor G. Craford.

N. Z. Hakim is with the Center for Telecommunications Research, Department of Electrical Engineering, Columbia University, New York, NY 10027.

B. E. A. Saleh is with the Department of Electrical and Computer Engineering, University of Wisconsin, Madison, WI 53706.

M. C. Teich is with the Department of Electrical Engineering, Columbia University, New York, NY 10027 and with the Department of Electrical and Computer Engineering, University of Wisconsin, Madison, WI 53706.

0018-9383/90/0300-0599$01.00 © 1990 IEEE

within each stage of the device. For a large number of substages, this variation may assume a continuous form. We have chosen this structure because of its generality. Special cases include the uniformly multiplying conventional APD [2], [3], [5], [9], [16]; the separate absorption/grading/multiplication (SAGM) APD [10], [17]; the multiquantum-well APD (MQW APD) [18]–[21]; and the staircase APD [4], [19], [22]–[24]. General expressions are derived for the mean multiplication and excess noise factors for dark-generated carriers alone, injected carriers alone, and for an arbitrary superposition of dark and injected carriers. The case of continuous carrier multiplication emerges as a special case of our results. Although the dark noise for multilayer APD's with two substages per stage was recently examined [25], the position-dependence of the carrier-pair generation within each stage was not accounted for.

The treatment presented here is based on a single-carrier initiated double-carrier multiplication process (SCIDCM), where it is specifically assumed that electrons initiate the avalanche process. Results for hole-initiated multiplication are obtained by simply interchanging the electron and hole ionization coefficients α and β. It is straightforward to convert the formulas into a form suitable for double-carrier initiated double-carrier multiplication (DCIDCM). The formalism follows the assumption that the ability of a carrier to ionize is independent of the carrier's history.

II. Model

The generalized multilayer structure examined in this paper is illustrated in Fig. 1. The depletion region of width w is represented by a spatial replication of an arbitrary number m of identical stages (three are shown in the figure). Each stage has total width L and consists of an arbitrary number N of substages (again, three are shown). Each substage is characterized by its width l, by constants α and β representing the electron- and hole-ionization coefficients, respectively, and by the rate at which dark carriers are generated g. These parameters vary from substage to substage, and their subscript designates their sequential position within each stage. The onset of a hypothetical avalanche process, arising from an initial dark-generated electron-hole pair generated at position x in the device, is shown by the solid and filled circles in Fig. 1 (these represent electrons and holes, respectively).

If the multiplication is continuous (but not necessarily uniform), α, β, and l are finite. For devices such as the ideal multiquantum-well and staircase APD's, however, certain limits for α, β, and l are appropriate. In those cases, a carrier-multiplication variance-to-mean ratio or Fano factor (constant within each substage) must be included. If $l \to 0$, for example, the Fano factor represents the reduction of noise for instantaneous Bernoulli multiplication. In the limit of an infinite number of stages, each of infinitesimal width, the results for the conventional APD are recovered from the model. These same results can, of course, also be obtained by modeling the entire depletion region as a single stage that itself consists of only a single substage.

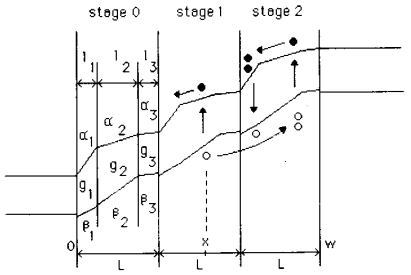

Fig. 1. Generalized multilayer structure used for the calculations presented in this paper. The depletion region is represented by a spatial replication of an arbitrary number m of identical stages ($m = 3$ is shown). Each stage has total width L and consists of an arbitrary number N of substages ($N = 3$ is shown). Each substage is characterized by its width l, by constants α and β representing the electron- and hole-ionization coefficients, respectively, and by the rate at which dark carriers are generated g. These parameters vary from substage to substage, and their subscript designates their sequential position within each stage. The onset of a hypothetical avalanche process, arising from an initial dark electron-hole pair generated at position x in the device, is shown by the solid and filled circles representing electrons and holes, respectively.

III. Theory

A. Calculation of the Mean Multiplication

The multiplication or gain noise (we use these terms interchangeably) of a conventional uniformly multiplying APD was first calculated by McIntyre in 1966 [2]. Our calculations make use of his general approach; however, we relax the restriction that the multiplication assume a Bernoulli form with infinitessimally small success probability in the limit of an infinitessimal distance.

Let $M(x)$ be the average number of electron-hole pairs resulting from an initial pair generated at position x in the depletion region (see Fig. 1). $M(x)$ represents the sum of all carrier pairs subsequently created: by electrons (solid circles) drifting to the left down the slope of potential energy and by holes (open circles) drifting to the right up the slope, in addition to the original pair. Thus $M(x)$ is given by

$$M(x) = 1 + \int_0^x \alpha(x')\, M(x')\, dx' + \int_x^w \beta(x')\, M(x')\, dx' \qquad (1)$$

provided that the ionization history of the carrier is ignored [2]. Differentiation provides

$$\frac{dM(x)}{dx} = [\alpha(x) - \beta(x)]\, M(x) \qquad (2)$$

which can be solved for the nth stage (for which $nL \le x \le (n+1)L$) and then extended to the entire depletion region.

For each substage i of any given stage, we can define the distance between the beginning of that stage and the end of the ith substage

$$L_i = \sum_{j=1}^{i} l_j, \qquad i = 1, \cdots, N$$

with $L_0 = 0$. Within the ith substage of the nth stage ($nL + L_{i-1} \le x \le nL + L_i$), the solution of (2) becomes

$$M(x) = M(nL) \exp\left(\sum_{j=1}^{i-1} (\alpha_j - \beta_j) l_j\right) \cdot \exp\left[(\alpha_i - \beta_i)(x - nL - L_{i-1})\right] \quad (3)$$

where the α_i and β_i are constant within any substage. For $x = (n + 1) L$ we immediately deduce

$$M((n + 1)L) = M(nL) \exp\left[\sum_{i=1}^{N} (\alpha_i - \beta_i) l_i\right]$$

and therefore, equivalently

$$\frac{M(nL)}{M((n + 1)L)} = \exp\left(\sum_{i=1}^{N} \beta_i l_i\right) \Big/ \exp\left(\sum_{i=1}^{N} \alpha_i l_i\right). \quad (4a)$$

We now proceed to several definitions that will permit us to compactly express our results for identical stages. Let

$$P = \exp\left(\sum_{i=1}^{N} \alpha_i l_i\right) - 1; \qquad Q = \exp\left(\sum_{i=1}^{N} \beta_i l_i\right) - 1.$$

If P and Q are less than unity, they represent the electron and hole ionization probabilities per stage, respectively [23]. Although we have assumed that all stages are identical, our analysis can be extended in a straightforward manner by permitting P and Q to be indexed by the stage number, thereby allowing them to differ from stage to stage. Alternatively, the entire depletion region can be considered in terms of a single stage, allowing for the most general structure.

Furthermore, we define the ionization-rates ratio k as $k = Q/P$. Depending on the limit in which our results are evaluated, k reduces to either the conventional APD ionization-rate ratio k_c or the multilayer ionization rate ratio k_s [1]. Equation (4a) can now be reexpressed as

$$\frac{M(nL)}{M((n + 1)L)} = \frac{1 + Q}{1 + P} = \frac{1 + kP}{1 + P} \triangleq R \quad (4b)$$

where R is a parameter that depends only on the fundamental quantities α and β and on the geometry of the depletion region. Converting (4b) to a recursion equation, with $M(mL) = M(w) = \langle M_e \rangle$, gives rise to

$$M(nL) = M(w) R^{m-n} \quad (5)$$

where w is the width of the depletion region. This result is similar to that derived by others [26].

For photocarriers injected at w, the multiplication $M(w)$ is precisely the standard mean multiplication of the device $\langle M_e \rangle$ which can, of course, be calculated from (1):

$$\langle M_e \rangle = 1 + \int_0^w \alpha(x) M(x)\, dx = 1 + \sum_{n=0}^{m-1} \sum_{i=1}^{N} \int_{nL + L_{i-1}}^{nL + L_i} \alpha_i M(x)\, dx.$$

Using (3), we obtain

$$\langle M_e \rangle = 1 + \sum_{n=0}^{m-1} M(nL) \sum_{i=1}^{N} \frac{\alpha_i}{\beta_i - \alpha_i} H_i \quad (6)$$

where $[H_i]$ represents a family of constants defined as

$$H_i = \exp\left[\sum_{j=1}^{i-1} (\alpha_j - \beta_j) l_j\right] \cdot \left\{1 - \exp\left[(\alpha_i - \beta_i) l_i\right]\right\}. \quad (7)$$

Like R, the parameter H_i depends only on α and β (and thereby on the external reverse bias) and on the structure of the depletion region. They will be used extensively in the upcoming formulas.

Using (5) and (7) in (6), we obtain

$$\frac{1}{\langle M_e \rangle} = 1 - \frac{R(1 - R^m)}{1 - R} \sum_{i=1}^{N} \frac{\alpha_i}{\beta_i - \alpha_i} H_i$$

so that

$$\langle M_e \rangle = \frac{1}{1 - \dfrac{R(1 - R^m)}{1 - R} \displaystyle\sum_{i=1}^{N} \frac{\alpha_i}{\beta_i - \alpha_i} H_i}. \quad (8)$$

Equation (8) represents the mean multiplication for injected electrons in the general multilayer structure presented in Fig. 1.

The dark generated carriers multiply differently because of their random spatial origin in the depletion region. The mean dark multiplication is defined as

$$\langle M_d \rangle = \frac{\displaystyle\int_0^w g(x) M(x)\, dx}{\displaystyle\int_0^w g(x)\, dx} = \frac{\displaystyle\sum_{n=0}^{m-1} \sum_{i=1}^{N} \int_{nL + L_{i-1}}^{nL + L_i} g_i M(x)\, dx}{m \displaystyle\sum_{i=1}^{N} g_i l_i}. \quad (9)$$

Using (3) and (5), (9) becomes

$$\langle M_d \rangle = \frac{\displaystyle\sum_{n=0}^{m-1} \sum_{i=1}^{N} g_i M(nL) \exp\left[\sum_{j=1}^{i-1} (\alpha_j - \beta_j) l_j\right] \left[1 - \exp(\alpha_i - \beta_i) l_i\right] \Big/ (\beta_i - \alpha_i)}{m \displaystyle\sum_{i=1}^{N} g_i l_i}$$

which can be more compactly expressed in terms of $\langle M_e \rangle$, using (5) and (7), as

$$\langle M_d \rangle = \langle M_e \rangle \frac{\dfrac{R(1 - R^m)}{1 - R} \displaystyle\sum_{i=1}^{N} \frac{g_i}{\beta_i - \alpha_i} H_i}{m \displaystyle\sum_{i=1}^{N} g_i l_i}. \quad (10)$$

Equations (4b), (7), (8), and (10) provide a full characterization of the mean multiplication of the generic multilayer device both for injected carriers and for carrier pairs generated throughout the depletion region.

The behavior of the mean dark multiplication is quite different in the two cases, as is illustrated in Fig. 2. Plots of $\langle M_d \rangle$ versus $\langle M_e \rangle$ for a conventional APD and for a five-stage MQW APD are presented in Fig. 2(a) and (b), respectively. The curves fall below the diagonal, indicating that the mean multiplication is reduced when the carriers are uniformly generated in the depletion region. This is, of course, expected inasmuch as the average carrier traverses only a limited portion of the depletion region and therefore undergoes only partial multiplication. Only for the conventional APD with $k_c = 1$ does $\langle M_d \rangle = \langle M_e \rangle$. In this case, the electron and hole ionization coefficients are equal so that an initial carrier pair will experience the same multiplication wherever it is generated. Comparing Fig. 2(a) and (b) shows that, for a given value of k, the mean dark multiplication is higher in the MQW APD than it is in the conventional APD. This is because electrons generated at an arbitrary position within a given stage experience full multiplication at the edge of that stage for the MQW APD but only partial multiplication (depending on the precise position of generation) for the conventional APD.

In the general case, both dark-generated and injected carriers exist. These give rise to the currents I_d and I_e, respectively. We therefore define a pre-multiplication mixed injection current $I_m = I_e + I_d$, which leads to a total multiplied current $I = I_m \langle M_m \rangle = I_e \langle M_e \rangle + I_d \langle M_d \rangle$, where $\langle M_m \rangle$ is the mean mixed multiplication. We also define the ratio of mean dark-generated to mean injected primary currents as $r = I_d/I_e$.

B. Calculation of the Current

The current consists of two components: the electron current I_n, which increases monotonically going "downhill" in the depletion region, and the hole current I_p, which increases monotonically going "uphill" in the depletion region (see Fig. 1). Because electrons and holes are created in pairs, an increase in the electron number is always accompanied by an increase in the hole number.

If we provide, in analogy with (1), that the increase in the hole current in an infinitesimal length dx at point x is the sum of the multiplied electron current and the multiplied hole current in that region plus the current associated with dark generation [2], we obtain

$$dI_p = (\alpha I_n + \beta I_p + g)\, dx. \quad (11)$$

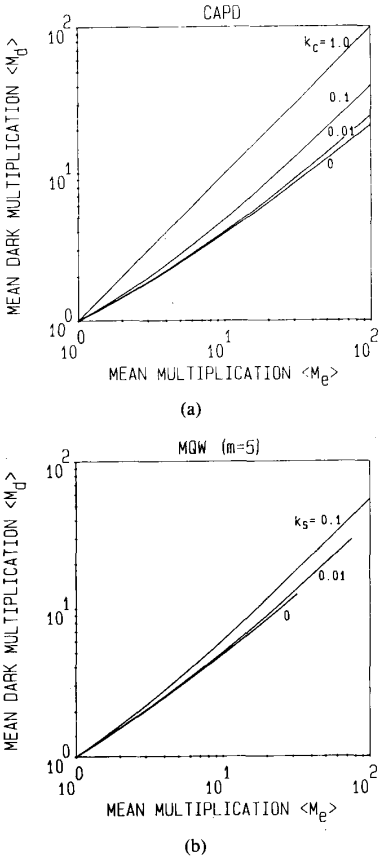

Fig. 2. (a) Mean dark multiplication $\langle M_d \rangle$ versus mean multiplication $\langle M_e \rangle$ for various values of the parameter k_c in a conventional APD (CAPD); (b) mean dark multiplication $\langle M_d \rangle$ versus mean multiplication $\langle M_e \rangle$ for various values of the parameter k_s in a five-stage MQW APD.

Furthermore, at any point x in the depletion region, the total current is constant and independent of x:

$$I_n(x) + I_p(x) = I$$

or equivalently

$$dI_n = -dI_p.$$

Using this in (11) leads to

$$\frac{dI_n}{dx} = (\beta - \alpha)\, I_n - (\beta I + g) \quad (12)$$

which can be solved within a particular stage ($nL \le x \le (n + 1)L$) and for the different substages within this stage.

For substage 1 in stage n ($nL \le x \le nL + L_1$), we obtain

$$I_n(x) = \left[I_n(nL) - \frac{\beta_1 I + g_1}{\beta_1 - \alpha_1} \right] \cdot \exp\left[(\beta_1 - \alpha_1)(x - nL)\right] + \frac{\beta_1 I + g_1}{\beta_1 - \alpha_1}.$$

Similarly in substage 2 of the nth stage ($nL + L_1 \leq x \leq nL + L_2$)

$$I_n(x) = \Bigg\{ I_n(nL) \exp\left[(\beta_1 - \alpha_1) l_1\right] - \frac{\beta_1 I + g_1}{\beta_1 - \alpha_1}\left[\exp\left((\beta_1 - \alpha_1) l_1\right) - 1\right] - \frac{\beta_2 I + g_2}{\beta_2 - \alpha_2}\Bigg\} \exp\left[(\beta_2 - \alpha_2)(x - nL - L_1)\right] + \frac{\beta_2 I + g_2}{\beta_2 - \alpha_2}.$$

In general, for substage i in the nth stage, the general expression for the current is

$$I_n(x) = \Bigg\{ I_n(nL) \exp\left[\sum_{j=1}^{i-1} (\beta_j - \alpha_j) l_j\right] - \sum_{j=1}^{i-1} \frac{\beta_j I + g_j}{\beta_j - \alpha_j}\left[\exp\left((\beta_j - \alpha_j) l_j\right) - 1\right] \cdot \exp\left[\sum_{k=j+1}^{i-1} (\beta_k - \alpha_k) l_k\right] - \frac{\beta_i I + g_i}{\beta_i - \alpha_i}\Bigg\} \cdot \left[\exp\left((\beta_i - \alpha_i)(x - nL - L_{i-1})\right]\right] + \frac{\beta_i I + g_i}{\beta_i - \alpha_i}. \tag{13}$$

Letting $i = N$ and $x = (n + 1) L$, we deduce that

$$I_n\big((n + 1)L\big) = I_n(nL) \exp\left[\sum_{i=1}^{N} (\beta_i - \alpha_i) l_i\right] - \sum_{i=1}^{N-1} \frac{\beta_i I + g_i}{\beta_i - \alpha_i}\left[\exp\left((\beta_i - \alpha_i) l_i\right) - 1\right] \cdot \exp\left[\sum_{j=i+1}^{N} (\beta_j - \alpha_j) l_j\right] - \frac{\beta_N I + g_N}{\beta_N - \alpha_N}\left[\exp\left((\beta_N - \alpha_N) l_N\right) - 1\right].$$

Rewriting this equation in terms of R and H_i ($i = 1, \cdots, N$), we obtain

$$I_n\big((n + 1)L\big) = I_n(nL) R - R \sum_{i=1}^{N} \frac{\beta_i I + g_i}{\beta_i - \alpha_i} H_i. \tag{14}$$

This equation can now be solved recursively by specifying the current at the edge of the depletion region. Under conditions of electron injection only, $I_n(w) = I_n(mL) = I_e$. This results in

$$I_n(nL) = \frac{R(1 - R^{n-m})}{R - 1} \sum_{i=1}^{N} \frac{\beta_i I + g_i}{\beta_i - \alpha_i} H_i + R^{n-m} I_e. \tag{15}$$

Equations (13) and (15) characterize the total electron current in the depletion region. The total current I is simply

$$I = I_e \langle M_e \rangle + I_d \langle M_d \rangle.$$

Alternatively, I can be obtained by solving (15) at $x = 0$, where $I_n(0) = I$; this calculation will not be carried out here.

C. Spectral Noise Density and Excess Noise Factor

The multiplication noise in APD's is characterized by the excess noise factor. For an arbitrary random variable M, this quantity is defined as the ratio of the second moment to the square of the first moment, i.e.

$$F = \frac{\langle M^2 \rangle}{\langle M \rangle^2}.$$

Using the relationship between the excess noise factor and the current spectral density obtained by Teich *et al.* [1, eq. (10c)], we find

$$S_m = 2e \langle I_m \rangle \langle M_m \rangle^2 \left[\underline{F}_a + (F_m - 1)\right]. \tag{16}$$

Here, $\langle I_m \rangle$ is the mean total current before multiplication, $\underline{F}_a$ is the *photon* Fano factor (ratio of variance to mean) for the incident light, and F_m is the excess noise factor associated with the mixed multiplication process

$$F_m = \frac{\langle M_m^2 \rangle}{\langle M_m \rangle^2}. \tag{17}$$

In the absence of dark current ($r = 0$), S_m and F_m reduce to the results for pure electron injection (S_e and F_e, respectively), whereas in the absence of injected current ($r = \infty$), they reduce to the results for pure dark generation (S_d and F_d, respectively).

We assume henceforth that the statistical properties of the carrier-pair generation process is Poisson, in which case $\underline{F}_a = 1$, and (16) reduces to

$$S_m = 2e \langle I_m \rangle \langle M_m \rangle^2 F_m. \tag{18}$$

We now proceed to calculate the spectral noise density in the general case in which there is a mixture of injected and dark-generated carriers. The expressions for S_e and S_d then obtain as special cases. The spectral noise component arising from the region between x and $x + dx$ is

$$dS_m = 2eM^2(x) \operatorname{var}\left(dI_p(x)\right) = 2eM^2(x)\, dI_p(x)\, \underline{F}(x) \tag{19}$$

where $\underline{F}(x)$ is the Fano factor associated with the multiplication $M(x)$ at position x. Using (11) we obtain

$$dS_m = 2eM^2(x)\left[(\alpha - \beta)\, I_n(x) + (\beta I + g)\right]\underline{F}\, dx. \tag{20}$$

Integrating this expression over the entire depletion region leads to

$$\begin{aligned} S_m &= 2e \int_0^w M^2(x)\left[(\alpha - \beta)\, I_n(x) + (\beta I + g)\right]\underline{F}\, dx \\ &= 2e \sum_{n=0}^{m-1} \sum_{i=1}^{N} \int_{nL+L_{i-1}}^{nL+L_i} M^2(x)\left[(\alpha_i - \beta_i)\, I_n(x)\right. \\ &\quad \left. + (\beta_i I + g_i)\right]\underline{F}_i\, dx. \end{aligned} \tag{21}$$

After substantial algebra, using (3), (4b), (7), and (13) in (21), we finally obtain

$$\begin{aligned} \frac{S_m}{2e} &= \langle M_e\rangle^2 I_e\left(1 - \frac{R(1-R^m)}{1-R}\sum_{n=1}^{N} H_n\underline{F}_n\right) \\ &\quad + \langle M_e\rangle^2 \frac{R(1-R^m)}{(1-R)}\sum_{n=1}^{N}\frac{\beta_n I + g_n}{\beta_n - \alpha_n} \\ &\quad \cdot H_n\left\{\frac{R}{R-1}\sum_{i=1}^{N} H_i\underline{F}_i - \frac{R(1+R^m)}{1+R}\right. \\ &\quad \cdot\left[\frac{R}{R-1}\sum_{i=1}^{N} H_i\underline{F}_i - \exp\left(\sum_{i=1}^{n-1}(\alpha_i - \beta_i)\, l_i\right)\right. \\ &\quad \left.\left. - \sum_{i=n+1}^{N} H_i\right]\right\}. \end{aligned} \tag{22a}$$

This is the principal result of this paper. It represents the noise spectral density for a generic multilayer APD in the presence of both injected and dark-generated carriers.

In the absence of dark current ($g_i = 0$, $i = 1, \cdots, N$) and for continuous (Bernoulli with infinitesimally small success probability P) multiplication ($\underline{F}_i = 1$, $i = 1, \cdots, N$), (22a) reduces to

$$\begin{aligned} \frac{S_e}{2e} &= \langle M_e\rangle^2 I_e(2 - R^m) + \frac{R(1-R^m)}{1-R} \\ &\quad \cdot \langle M_e\rangle^3 I_e \sum_{n=1}^{N}\frac{\beta_n H_n}{\beta_n - \alpha_n}\left\{1 - \frac{R(1+R^m)}{1+R}\right. \\ &\quad \left.\cdot\left[\sum_{i=1}^{n-1} H_i - \sum_{i=n+1}^{N} H_i\right]\right\} \end{aligned} \tag{22b}$$

which is a generalization of the McIntyre formula [2] applicable for an arbitrary depletion region structure. On the other hand, in the presence of dark current alone ($I_e = 0$) and for continuous (Bernoulli with infinitesimally small success probability P) multiplication, (22a) becomes

$$\begin{aligned} \frac{S_d}{2e} &= \langle M_e\rangle^2 \frac{R(1-R^m)}{1-R}\sum_{i=1}^{N}\frac{\beta_i I + g_i}{\beta_i - \alpha_i} H_i \\ &\quad \cdot\left[1 - \frac{R(1+R^m)}{1+R}\left(\sum_{j=1}^{i-1} H_j - \sum_{j=i+1}^{N} H_j\right)\right]. \end{aligned} \tag{22c}$$

In those cases in which α, β, and g are continuous and differentiable functions of position in the depletion region, which are denoted $\alpha(x)$, $\beta(x)$, and $g(x)$, respectively, the number of substages per stage $N \to \infty$ and the Fano factor $\underline{F}$ becomes unity, whereupon the spectral noise density in (22a) assumes a simpler form. For the substage i containing the point x ($0 \le x \le L$), the parameters H_i defined in (7) take the form $H(x)\, dx$ in the limiting case where $l_i = dx$, i.e.

$$\begin{aligned} H_i &= \exp\left[\sum_{j=1}^{i-1}(\alpha_j - \beta_j)\, l_j\right]\left\{1 - \exp\left[(\alpha_i - \beta_i)\, l_i\right]\right\} \\ &\to \left[\beta(x) - \alpha(x)\right]\exp\left\{\int_0^x\left[\alpha(x') - \beta(x')\right]dx'\right\}\cdot dx \\ &= H(x)\, dx. \end{aligned} \tag{23}$$

Similarly, replacing the sum by an integral in (4a) provides

$$R = \exp\left\{\int_0^L\left[\beta(x') - \alpha(x')\right]dx'\right\} \tag{24}$$

whereupon (22a) becomes

$$\begin{aligned} \frac{S_m}{2e} &= \langle M_e\rangle^2 I_e\left\{1 - \frac{R(1-R^m)}{1-R}\int_0^L H(x)\, dx\right\} \\ &\quad + \langle M_e\rangle^2 \frac{R(1-R^m)}{(1-R)}\int_0^L \frac{\beta I + g}{\beta - \alpha} H(x)\, dx \\ &\quad \cdot\left\{\frac{R}{R-1}\int_0^L H(x)\, dx\right. \\ &\quad - \frac{R(1+R^m)}{1+R}\cdot\left[\frac{R}{R-1}\int_0^L H(x')\, dx'\right. \\ &\quad \left.\left. - \exp\left(\int_0^x(\alpha - \beta)\, dx'\right) - \int_x^L H(x)\, dx\right]\right\} \end{aligned} \tag{22d}$$

in the continuous limit. This result is a version of the expression obtained by McIntyre that incorporates both injected and dark-generated carriers [2].

We now proceed to evaluate this quantity for a number of multilayer and conventional structures of interest.

IV. Application to Specific Avalanche Photodiodes

A. Conventional Avalanche Photodiode (CAPD)

The generic model illustrated in Fig. 1 becomes the conventional APD (CAPD), with parameters α, β, and g, if there is only one substage per stage ($N = 1$). These results are obtained by taking the number of stages $m \to \infty$ with the ionization probabilities $P \to 0$, $Q \to 0$ [1], [19], [23], [27]. In this limit, P and Q become

$$P = [\exp(\alpha L) - 1] \approx \alpha L$$

$$Q = [\exp(\beta L) - 1] \approx \beta L.$$

The ionization-coefficient ratio k therefore becomes

$$k_c = \frac{Q}{P} = \frac{\beta}{\alpha}$$

so that

$$R = \exp[(\beta - \alpha)L]$$

and since $mL \to w$

$$R^m = e^{-\alpha w(1-k_c)}.$$

Similarly,

$$H_1 = 1 - e^{(\alpha-\beta)L} = 1 - 1/R$$

and

$$\underline{F}_1 = 1.$$

The mean multiplication $\langle M_e \rangle$ is obtained by using these results in (8) and (10) with $I_d = gw$

$$\langle M_e \rangle = \frac{1}{1 - \dfrac{1 - R^m}{1 - k_c}} = \frac{1 - k_c}{e^{-\alpha w(1-k_c)} - k_c}, \qquad k_c \neq 1 \tag{25}$$

in accordance with [1, eq. (18)]. For $k_c = 1$, $\langle M_e \rangle = 1/(1 - \alpha w)$. Similarly, $\langle M_d \rangle$ is obtained by substitution in (10):

$$\langle M_d \rangle = \langle M_e \rangle \frac{R(1 - R^m)}{I_d(1 - R)} \frac{g}{\alpha - \beta} H_1$$

$$= \langle M_e \rangle (1 - R^m)/\alpha w(1 - k_c)$$

or

$$\langle M_d \rangle = \frac{1}{\alpha w} \frac{1 - e^{-\alpha w(1-k_c)}}{e^{-\alpha w(1-k_c)} - k_c}, \qquad k_c \neq 1. \tag{26}$$

A comparison between (25) and (26) permits us to obtain the mean dark multiplication in terms of the mean injected multiplication for the conventional APD, i.e.

$$\langle M_d \rangle = \frac{1}{\alpha w}(\langle M_e \rangle - 1). \tag{27}$$

The noise spectral density S_d arising from dark-generated events, from (22c), is

$$S_d = 2e\langle M_e \rangle^2 \frac{\beta I + g}{\beta - \alpha} H_1 \frac{R(1 - R^m)}{1 - R}.$$

Using (10) and (27), we obtain

$$S_d = 2eI_d \langle M_e \rangle \langle M_d \rangle (1 + k_c \alpha w \langle M_d \rangle), \tag{28}$$

the last term of which is precisely that arising from hole injection multiplication $M(0)$ of the conventional APD [2], which we denote by $\langle M_h \rangle$. This corresponds to the generation of photocarriers at the point $x = 0$ in the depletion region so that only holes initiate the avalanche process. This result is equivalent to that obtained by considering the conventional APD to be a structure with an infinite number of stages ($m \to \infty$) and with a single substage ($N = 1$), i.e., the continuous limit (22d).

The expression for the conventional APD dark excess noise factor is therefore

$$F_d = \frac{\langle M_e \rangle \langle M_h \rangle}{\langle M_d \rangle}$$

$$= \frac{(1 + \alpha w \langle M_d \rangle)(1 + k_c \alpha w \langle M_d \rangle)}{\langle M_d \rangle}. \tag{29}$$

which is in agreement with [6]–[8]. The dark excess noise factor F_d versus the mean dark multiplication $\langle M_d \rangle$, with k_c as a parameter, is presented in Fig. 3(a). A similar approach using (22b) for electron injection provides the noise spectral density S_e and the well known excess noise factor F_e, which is shown in Fig. 3(b).

For any given value of k_c except unity, the dark excess noise factor F_d increases more rapidly with the mean dark multiplication than does the excess noise factor F_e with the mean electron multiplication. This arises from the additional randomness in the generation positions of the dark-generated carriers. More generally, the case of mixed injection is shown in Fig. 3(c) for various values of dark-to-injected current ratio r when $k_c = 10^{-3}$. When $r = 0$ and $r = \infty$, we recover the pure injection and pure dark-generated results, respectively. For intermediate values of r, the excess noise factor lies between these two limiting values. The same results can be obtained by appealing directly to the continuous-limit result (22d).

B. Multiquantum-Well Avalanche Photodiode (MQW APD)

The MQW APD has been discussed by a number of authors [18]–[21]. Its band diagram is represented in Fig. 4 in terms of the generic multilayer band structure shown in Fig. 1. Only three stages ($m = 3$) are shown for simplicity. Each stage comprises three substages ($N = 3$). The idealized MWQ APD band structure emerges in the limits $l_1 \to 0$, $\alpha_1 \to \infty$, $\underline{F}_1 = 1 - P$; $l_2 = L/2$, $\alpha_2 = 0$, $g_2 = 0$, $\underline{F}_2 = 1$; $l_3 = L/2$, $\alpha_3 = 0$, $g_3 = g$, $\underline{F}_3 = 1$; $\beta_2 = \beta_3 = \beta$. Because $l_1 \to 0$, dark counts and hole ioniza-

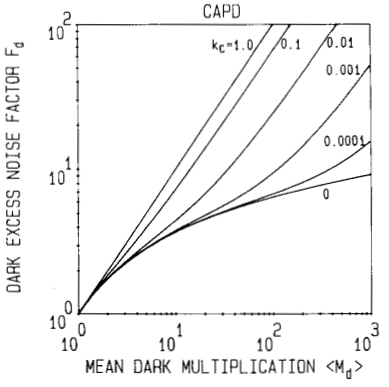

Fig. 3. (a) Variation of the dark excess noise factor F_d versus the mean dark multiplication $\langle M_d \rangle$ for a conventional APD with k_c as a parameter; (b) variation of the excess noise factor F_e versus mean multiplication $\langle M_e \rangle$ for the same structure shown in (a). The randomness in the positions of the dark carrier-pair generations in (a) results in greater noise than in the injected carrier case. (c) Variation of the mixed excess noise factor F_m versus mean mixed multiplication $\langle M_m \rangle$ for the same structure shown in (a). The parameter r represents the ratio of (unmultiplied) dark to injected currents. The results are intermediate between those shown in (a) and (b).

tions do not arise in this region; thus, the dark generation *rate* g_1 and hole generation *rate* β_1 may take on arbitrary finite values.

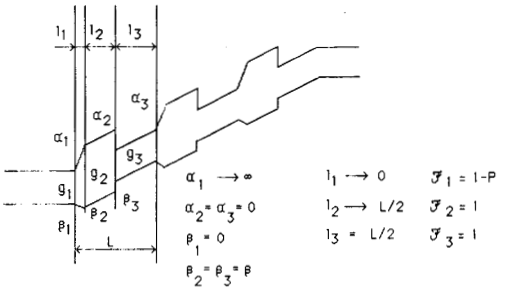

Fig. 4. Band diagram of a MQW APD represented in terms of the generic multilayer band structure shown in Fig. 1. Only three stages ($m = 3$), each consisting of three substages ($N = 3$), are shown for simplicity. This particular sequence of substages, which would not be used in practice because of the presence of an initial barrier, was chosen to be compatible with our earlier results [1]. The idealized MQW APD band structure emerges in the limits indicated in the figure.

The principal contribution to the dark current is assumed to arise in the third substage, where the bandgap is smallest.

Under these conditions, (7) gives rise to the following values for H:

$$H_1 = 1 - \exp\left[(\alpha_1 - \beta_1) l_1\right] \to 1 - \exp(\alpha_1 l_1) = -P$$

$$H_2 = (1 + P)\left(1 - \frac{1}{(1 + k_s P)^{1/2}}\right)$$

and

$$H_3 = \frac{1 + P}{(1 + k_s P)^{1/2}}\left(1 - \frac{1}{(1 + k_s P)^{1/2}}\right).$$

Substituting these results into (8), and making use of (4b), provides

$$\langle M_e \rangle = \frac{1}{1 - P\dfrac{R(1 - R^m)}{1 - R}} = \frac{(1 + P)^m (1 - k_s)}{(1 + k_s P)^{m+1} - k_s (1 + P)^{m+1}} \quad (30)$$

which is identical to [1, eq. (27)], as expected.

Similarly, using (10) for the dark-current multiplication leads to

$$\langle M_d \rangle = \langle M_e \rangle \frac{\dfrac{R(1 - R^m)}{1 - R} H_3/\beta}{mL/2} = 2\langle M_e \rangle \frac{\dfrac{R(1 - R^m)}{1 - R} H_3}{m\beta L}. \quad (31)$$

The relationship between β and Q

$$\beta L = \ln (1 + k_s P),$$

which reduces in the case of small k_s to

$$\beta L \approx k_s P$$

may be used.

The appropriate parameters for a ten-stage MQW APD can be inserted in (22a). The behavior of the dark excess noise factor F_d versus the mean dark multiplication $\langle M_d \rangle$ for a ten-stage MQW APD is illustrated in Fig. 5(a) with k_s as a parameter. The dark events were assumed to be generated only in the regions of low bandgap. The case of uniform generation throughout the depletion layer was also calculated; the results are indistinguishable from those shown in Fig. 5(a) within the graphical accuracy of the plot. The results in Fig. 5(a) are to be compared with those for the excess noise factor F_e versus mean multiplication $\langle M_e \rangle$, which is shown in Fig. 5(b). More generally, the case for mixed injection is shown in Fig. 5(c) for various values of dark-to-injected current ratio r, when $k_s = 10^{-3}$. When $r = 0$ and $r = \infty$, we recover the pure injection and pure dark-generated results, respectively. For intermediate values of r, the excess noise factor lies between these two limiting values. The same effect was seen with the conventional APD illustrated in Fig. 3(c). This result arises, of course, because of the added randomness associated with the dark carrier-pair generation process.

C. Staircase Avalanche Photodiode

The potential benefits of a staircase structure have been considered by a number of authors [4], [19], [22]–[24], although the growth of a structure involving graded gaps presents a substantial challenge. The dark noise associated with the staircase APD requires separate treatment because the bandgap varies with position within each stage of the device as does the dark generation rate $g(x)$.

The band diagram for the staircase APD is represented in Fig. 6(a) in terms of the generic multilayer band structure shown in Fig. 1. Only three stages ($m = 3$) are shown for simplicity. Each stage comprises two substages ($N = 2$). The idealized staircase band structure emerges in the limits $l_1 \to 0$, $\alpha_1 \to \infty$, with $\alpha l_1 = P$, $\underline{F}_1 = 1 - P$; $l_2 = L$, $\alpha(x) = 0$; $\beta_1 = \beta(x) = \beta$, $\underline{F}(x) = 1$ and is represented in Fig. 6(b). Electron-initiated multiplication is therefore assumed to occur only at the risers of the staircase, whereas hole-initiated multiplication is taken to have a constant ionization coefficient $\beta(x) = \beta$ throughout the depletion region. In the graded-bandgap region, $\underline{F}$ assumes the value 1, whereas at the edge, it becomes $(1 - P)$ to account for Bernoulli multiplication with finite success probability P.

The dark current is assumed to be generated throughout the graded region where the bandgap varies. The dark carrier pairs may be generated by two mechanisms: by the tunneling of electrons from the valence band into the conduction band or by the thermal excitation of electrons into

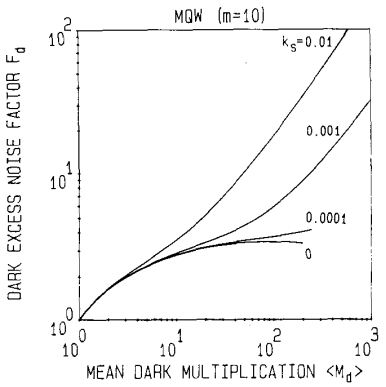

Fig. 5. (a) Variation of the dark excess noise factor F_d versus the mean dark multiplication $\langle M_d \rangle$ for a 10-stage MQW APD with k_s as a parameter. The values for l, α, β, and g are as shown in Fig. 4; (b) variation of the excess noise factor F_e versus mean multiplication $\langle M_e \rangle$ for the same structure shown in (a). The randomness in the positions of the dark carrier-pair generations in (a) results in a greater noise than in the injected carrier case. (c) Variation of the mixed excess noise factor F_m versus mean mixed multiplication $\langle M_m \rangle$ for the same structure shown in (a). The parameter r represents the ratio of (unmultiplied) dark to injected currents. The results are intermediate between those shown in (a) and (b).

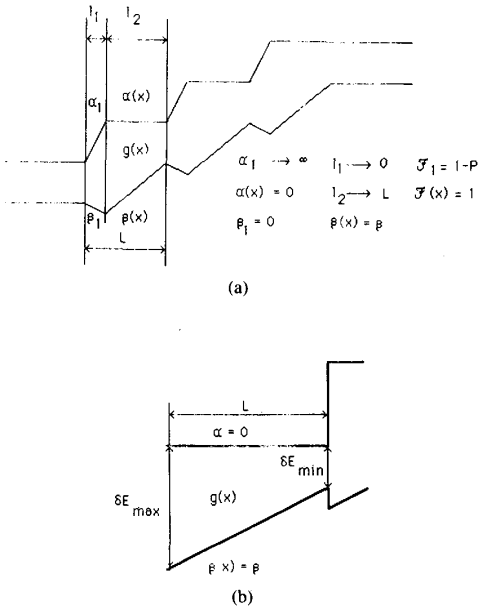

Fig. 6. (a) Band diagram of a staircase APD represented in terms of the generic multilayer band structure shown in Fig. 1. Only three stages ($m = 3$) are shown for simplicity. Each stage consists of two substages ($N = 2$). The idealized staircase band structure emerges in the limits indicated. (b) A single stage of the staircase structure is shown when the width of substage 1 has been reduced to 0. $g(x)$ is taken to represent the thermal dark generation rate in the continuous region. The maximum bandgap δE_{max} and the minimum bandgap δE_{min} used to calculate the multiplication noise in the device are indicated.

the conduction band. The dependence of the dark-generation rate on the bandgap differs in the two cases.

As a particular example, we consider the operation of a staircase structure that is assumed to be dominated by thermally generated dark carrier pairs. In this case, the dependence of g on the bandgap energy δE is described by [28]

$$g(T) = g(T = \infty) \exp(-\delta E/KT) \tag{32}$$

where K is Boltzmann's constant, and T is the temperature of the device. For a fixed temperature T, the thermal dark-generation rate can be written in terms of the local bandgap δE as (see Fig. 6(b))

$$g(\delta E) = g(\delta E_{max}) \exp\left(\frac{\delta E_{max} - \delta E}{kT}\right). \tag{33}$$

Assuming an ideal staircase APD in which the bandgap varies linearly with position within each stage, as is illustrated in Fig. 6(b), we rewrite (33) as

$$g(x) = g(nL^+) \exp\left[\frac{-(\delta E_{min} - \delta E_{max})}{LKT}(x - nL)\right]$$
$$= g_0 \exp\left[-G(x - nL)\right] \tag{34}$$

where g_0 is the dark-generation rate at the maximum bandgap $g(\delta E_{max})$ and

$$G = (\delta E_{min} - \delta E_{max})/LKT.$$

The dark current is then

$$I_d = \sum_{n=0}^{m-1} \int_{nL}^{(n+1)L} g(x)\, dx.$$

Using (34), we obtain

$$I_d = m g_0 G\left[1 - \exp(-GL)\right]. \tag{35}$$

At the step, the constant H_i becomes

$$H_1 = \lim\left[1 - \exp(\alpha_1 l_1)\right] = -P$$

whereas elsewhere, they are given by

$$H(x)\, dx = \exp(\alpha_1 l_1) \exp\left(\sum_{j=2}^{i-1} (\alpha_j - \beta_j)\, l_j\right) \cdot \left[1 - \exp(\beta_i - \alpha_i)\, l_i\right]$$
$$= (1 + P)\, \beta \exp\left[-\int_0^x \beta\, dx'\right] dx$$
$$= (1 + P)\, \beta \exp(-\beta x)\, dx. \tag{36}$$

Using (10), the mean dark multiplication $\langle M_d \rangle$ becomes

$$\langle M_d \rangle = \langle M_e \rangle \frac{\dfrac{R(1 - R^m)}{1 - R} \displaystyle\int_{0^+}^{L} dx\, g(x)\, H(x)/\beta}{m \displaystyle\int_0^L g(x)\, dx}$$

$$= \langle M_e \rangle \frac{\dfrac{R(1 - R^m)}{1 - R} \dfrac{(1 + P)\, g_0}{(\beta + G)} \left\{1 - \exp\left[-(\beta + g)L\right]\right\}}{m g_0 G\left[1 - \exp(-GL)\right]}. \tag{37}$$

so that

$$\frac{S_m}{2e} = \langle M_e \rangle^2 I_e \Bigg\{ 1 - \frac{R(1-R^m)}{1-R} \Bigg[-P(1-P) + \int_{0^+}^{L} H(x)\,dx \Bigg] \Bigg\} + \langle M_e \rangle^2 \frac{R(1-R^m)}{1-R} \int_{0^+}^{L} \frac{\beta I + g}{\beta - \alpha} \cdot H(x)\,dx \Bigg\{ \frac{R}{R-1} \Bigg[-P(1-P) + \int_{0^+}^{L} H(x')\,dx' \Bigg] - \frac{R(1+R^m)}{1+R} \Bigg[\frac{R}{R-1} \Bigg(-P(1-P) + \int_{0^+}^{L} H(x')\,dx' \Bigg) - \exp\left(\int_{0^+}^{x} (\alpha - \beta)\,dx' \right) - \int_{x}^{L} H(x')\,dx' \Bigg] \Bigg\}. \quad (38)$$

Replacing $g(x)$ and $H(x)$ by the expressions given in (34) and (36), respectively, leads to a formula for the mixed noise spectral density for the staircase APD. Although we have not plotted the excess noise factors for the staircase device, they are expected to closely resemble those for the MQW APD. This is because the plots for the excess noise factor of a ten-stage MQW APD with uniform dark carrier generation throughout the depletion region are indistinguishable (within the accuracy of the plot) from those presented in Fig. 5.

V. Conclusion

We have considered a generic multilayer avalanche photodiode model that admits arbitrary variation (with position) of the bandgap, dark generation rate, and ionization coefficients within each stage of the device. Expressions for the mean multiplication and excess noise factors for dark carriers alone, injected carriers alone, and for an arbitrary mixture of dark and injected carriers were obtained. Carriers that are photogenerated throughout the depletion region behave like dark-generated carriers. Our expressions reduce to the well known results for the conventional APD, the multiquantum-well APD, the staircase APD, and the separate absorption/grading/multiplication APD. In all cases, the excess noise factor for a multilayer APD lies below that for a conventional APD.

The treatment presented here is based on a single-carrier initiated double-carrier multiplication process (SCIDCM), where it is specifically assumed that electrons initiate the avalanche process. Results for hole-initiated multiplication are obtained by simply interchanging the electron and hole ionization coefficients α and β. Expressions for double-carrier initiated double-carrier multiplication (DCIDCM) are readily obtained from the formulas derived here by solving (14) subject to the condition $I_n(w) = I_e + \langle M_h \rangle I_h$.

Our formalism follows the usual assumption that the ability of a carrier to ionize other carriers is independent of the carrier's history. It will be useful to modify this assumption so that the carrier ionization coefficients $\alpha(x)$ and $\beta(x)$ become $\alpha(x, x')$ and $\beta(x, x')$, respectively, to reflect the ionization probabilities of a carrier at the point x when it was generated at the point x'. The simplest model to account for this type of behavior introduces a "dead space," which prohibits the carrier from multiplying within a certain distance of its birthplace, thereby reflecting the physical requirement that it gain sufficient energy to do so. We have recently obtained a number of results that incorporate the effects of dead space [29].

Acknowledgment

We are grateful to R. J. McIntyre for many useful suggestions.

References

[1] M. C. Teich, K. Matsuo, and B. E. A. Saleh, "Excess noise factors for conventional and superlattice avalanche photodiodes and photomultiplier tubes," *IEEE J. Quantum Electron.*, vol. QE-22, pp. 1184–1193, 1986.

[2] R. J. McIntyre, "Multiplication noise in uniform avalanche diodes," *IEEE Trans. Electron Devices*, vol. ED-13, pp. 164–168, 1966.

[3] R. J. McIntyre, "The distribution of gains in uniformly multiplying avalanche photodiodes: Theory," *IEEE Trans. Electron Devices*, vol. ED-19, pp. 703–713, 1972.

[4] F. Capasso, W. T. Tsang, and G. F. Williams, "Staircase solid-state photomultipliers and avalanche photodiodes with enhanced ionization rates ratio," *IEEE Trans. Electron Devices*, vol. ED-30, pp. 381–390, 1983.

[5] P. P. Webb, R. J. McIntyre, and J. Conradi, "Properties of avalanche photodiodes," *RCA Rev.*, vol. 35, pp. 234–278, 1974.

[6] N. Z. Hakim, M. C. Teich, and B. E. A. Saleh, "Dark-current multiplication and excess noise factor in conventional avalanche photodiodes," *J. Opt. Soc. Amer. A*, vol. 4, p. 123, 1987.

[7] C. Fujihashi, "Dark-current multiplication noises in avalanche photodiodes and optimum gains," *J. Lightwave Technol.*, vol. LT-5, pp. 798–808, 1987.

[8] R. S. Fyath and J. J. O'Reilly, "Performance degradation of APD-optical receivers due to dark current generated within the multiplication region," *J. Lightwave Technol.*, vol. 7, pp. 62–67, 1989.

[9] G. E. Stillman and C. M. Wolfe, "Avalanche photodiodes," in *Semiconductors and Semimetals, Infrared Detectors II*, R. K. Willardson and A. C. Beer, Eds. New York: Academic, 1977, vol. 12, pp. 291–394.

[10] J. C. Campbell, A. G. Dentai, W. S. Holden, and B. L. Kasper, "High-performance avalanche photodiode with separate absorption 'grading' and multiplication regions," *Electron. Lett.*, vol. 19, pp. 818–820, 1983.

[11] V. Diadiuk, S. H. Groves, and C. E. Hurwitz, "Avalanche multiplication and noise characteristics of low-dark-current GaInAsP/InP avalanche photodetectors," *Appl. Phys. Lett.*, vol. 37, pp. 807–809, 1980.

[12] K. Yasuda *et al.*, "InP/InGaAs buried-structure avalanche photodiodes," *Electron. Lett.*, vol. 20, pp. 158–159, 1984.

[13] D. O. Cummings, "Simulation of thermal noise at optical frequencies

and use of an avalanche photodiode for high speed photon counting," Ph.D. dissertation, Pennsylvania State University, State College, PA, 1972.
[14] K. Shimizu, M. Fujise, and M. Nunokawa, "Synchronous single-photon counting using an Si avalanche photodiode at room temperature," *Electron. Lett.*, vol. 23, pp. 1307-1308, 1987.
[15] R. G. W. Brown, K. D. Ridley, and J. G. Rarity, "Characterization of silicon avalanche photodiodes for photon correlation measurements. 1: Passive quenching," *Appl. Opt.*, vol. 25, pp. 4122-4126, 1986.
[16] K. M. Johnson, "High-speed photodiode signal enhancement at avalanche breakdown voltage," *IEEE Trans. Electron Devices*, vol. ED-12, pp. 55-63, 1965.
[17] B. L. Kasper, J. C. Campbell, and A. G. Dentai, "Measurements of the statistics of excess noise in separate absorption, grading and multiplication (SAGM) avalanche photodiodes," *Electron. Lett.*, vol. 20, pp. 796-798, 1984.
[18] R. Chin, N. Holonyak, G. E. Stillman, J. Y. Tang, and K. Hess, "Impact ionization in multilayered heterojunction structures," *Electron. Lett.*, vol. 16, pp. 467-469, 1980.
[19] K. Brennan, "Comparison of multiquantum well, graded barrier, and doped quantum well GaInAs/AlInAs avalanche photodiodes: A theoretical approach," *IEEE J. Quantum Electron.*, vol. QE-23, pp. 1273-1282, 1987.
[20] K. Brennan, "Calculated electron and hole spatial ionization profiles in bulk GaAs and superlattice avalanche photodiodes," *IEEE J. Quantum Electron.*, vol. 24, pp. 2001-2006, 1988.
[21] K. F. Brennan, Y. Wang, M. C. Teich, B. E. A. Saleh, and T. Khorsandi, "Theory of the temporal response of a simple multiquantum-well avalanche photodiode," *IEEE Trans. Electron Devices*, vol. 35, pp. 1456-1467, 1988.
[22] G. F. Williams, F. Capasso, and W. T. Tsang, "The graded bandgap multilayer avalanche photodiode: A new low-noise detector," *IEEE Electron Device Lett.*, vol. EDL-3, pp. 71-73, 1982.
[23] K. Matsuo, M. C. Teich, and B. E. A. Saleh, "Noise properties and time response of the staircase avalanche photodiode," *IEEE Trans. Electron Devices*, vol. ED-32, pp. 2615-2623, 1985 (see also *J. Lightwave Technol.*, vol. LT-3, pp. 1223-1231, 1985).
[24] F. Capasso, "Physics of avalanche photodiodes," in *Semiconductors and Semimetals*, R. K. Willardson and A. C. Beer, Eds. *Lightwave Communications Technology*, W. T. Tsang, Ed. New York: Academic, 1985, vol. 22, part D, pp. 1-172.
[25] R. S. Fyath and J. J. O'Reilly, "Multilayer APDs producing up to two impact ionisations per carrier per stage: Optical receiver performance analysis," *Proc. Inst. Elec. Eng.*, part J, vol. 135, pp. 101-108, 1988.
[26] J. J. O'Reilly and R. S. Fyath, "Analysis of the influence of dark current on the performance of optical receivers employing superlattice APDs," *Proc. Inst. Elec. Eng.*, part J, vol. 135, pp. 109-118, 1988.
[27] M. C. Teich, K. Matsuo, and B. E. A. Saleh, "Time and frequency response of the conventional avalanche photodiode," *IEEE Trans. Electron Devices*, vol. ED-33, pp. 1511-1517, 1986.
[28] S. Forrest, "Sensitivity of avalanche photodetector receivers for high-bit-rate long-wavelength optical communication systems," in *Semiconductors and Semimetals*, R. K. Willardson and A. C. Beer, Eds. *Lightwave Communications Technology*, W. T. Tsang, Ed. Academic: New York, 1985, vol. 22, part D, pp. 329-387.
[29] B. E. A. Saleh, M. M. Hayat, and M. C. Teich, "Effect of dead space on the excess noise factor and time response of avalanche photodiodes," submitted for publication.

*

Nagib Z. Hakim (S'87) received the Diplôme d'Ingénieur degree from St. Joseph University, Beirut, Lebanon, and the M.S. degree from Columbia University, in 1985 and 1986, respectively, both in electrical engineering. He is currently working toward the Ph.D. degree at the Center for Telecommunications Research, Department of Electrical Engineering, Columbia University.

His research interests include the modeling and control of communication networks and theoretical and applied studies of neural networks.

Bahaa E. A. Saleh (M'73-SM'86) received the B.S. degree from Cairo University, Cairo, Egypt, in 1966 and the Ph.D. degree from the Johns Hopkins University, Baltimore, MD, in 1971, both in electrical engineering.

From 1971 to 1974, he was an Assistant Professor at the University of Santa Catarina, Brazil. Thereafter, he joined the Max Planck Institute in Goettingen, Germany, where he was involved in the research of laser light scattering and photon correlation spectroscopy. He is presently Professor of Electrical and Computer Engineering at the University of Wisconsin, Madison, where he has been since 1977. He held visiting appointments at the University of California, Berkeley, in 1977, and the Columbia Radiation Laboratory of Columbia University, New York, NY in 1983. He is currently involved in the research of image processing, optical information processing, statistical optics, optical communication, and vision. He is the author of *Photoelectron Statistics* (Springer, 1978) and a co-editor of *Transformations in Optical Signal Processing* (SPIE, 1981). During 1980-1983, he was an associate editor of the *Journal of the Optical Society of America*, and during 1983-1988, he was a topical editor of the same journal. He is a member of the Board of Editors of *Quantum Optics*.

Dr. Saleh is is a Fellow of the Optical Society of America and a member of Phi Beta Kappa and Sigma Xi. He received the Wisconsin Romnes Award in 1981 and was appointed a Guggenheim Fellow in 1984.

*

Malvin C. Teich (S'62-M'66-SM'72-F'89) was born in New York City. He received the S.B. degree in physics from the Massachusetts Institute of Technology, Cambridge, MA, in 1961, the M.S. degree in electrical engineering from Stanford University, Stanford, CA, in 1962, and the Ph.D. degree in quantum electronics from Cornell University, Ithaca, NY, in 1966.

In 1966, he joined the MIT Lincoln Laboratory, Lexington, MA, where he was engaged in work on coherent infrared detection. In 1967, he became a member of the faculty in the Department of Electrical Engineering, Columbia University, New York, NY where he is now teaching and pursuing his research interests in the areas of quantum optics, optical and infrared detection, and sensory perception. He served as Chairman of the Department from 1978 to 1980. He is also a member of the faculty in the Department of Applied Physics and a member of the Columbia Radiation Laboratory, the Center for Telecommunications Research, and the Fowler Memorial Laboratory at the Columbia College of Physicians and Surgeons. He has authored or coauthored some 150 technical publications and holds one patent.

Dr. Teich was the recipient of the IEEE Browder J. Thompson Memorial Prize Award for his paper "Infrared Heterodyne Detection," in 1969 and in 1981, he received a Citation Classic Award of the Institute for Scientific Information for this work. He received a Guggenheim Fellowship in 1973. He is a Fellow of the American Physical Society, the Optical Society of America, and the American Association for the Advancement of Science. He is a member of Sigma Xi, Tau Beta Pi, the Acoustical Society of America, and the Association for Research in Otolaryngology. He served as a member of the Editorial Advisory Panel for the journal *Optics Letters* from 1977 to 1979 and is currently Deputy Editor of the journal *Quantum Optics* and a member of the Editorial Board of the *Journal of Visual Communication and Image Technology*.